









RESEARCH ARTICLE

Raman spectroscopy is sensitive to biochemical changes related to various cartilage injuries

Rubina Shaikh^{1,2}  | Ervin Nippolainen^{1,2}  | Vesa Virtanen³  |
 Jari Torniainen¹  | Lassi Rieppo³  | Simo Saarakkala^{3,4}  |
 Isaac O. Afara^{1,5}  | Juha Töyräs^{1,5,6} 

¹Department of Applied Physics, University of Eastern Finland, Kuopio, Finland

²Department of Orthopedics Traumatology and Hand Surgery, Kuopio University Hospital, Kuopio, Finland

³Research Unit of Medical Imaging, Physics and Technology, University of Oulu, Oulu, Finland

⁴Department of Diagnostic Radiology, Oulu University Hospital, Oulu, Finland

⁵School of Information Technology and Electrical Engineering, The University of Queensland, Brisbane, Australia

⁶Diagnostic Imaging Centre, Kuopio University Hospital, Kuopio, Finland

Correspondence

Rubina Shaikh, Ph.D., Department of Applied Physics, University of Eastern Finland, Finland, P.O. Box 1627, 70211. Kuopio, Finland.
 Email: rubinas@uef.fi

Funding information

Academy of Finland, Grant/Award Number: 315820; Doctoral Programme in Science, Technology, and Computing (SCITECO) of University of Eastern Finland; Kuopio University Hospital, Grant/Award Number: 5203111; The MIRACLE project-Horizon 2020 research and innovation programme-H2020-ICT-2017-1, Grant/Award Number: 780598

Abstract

Raman spectroscopy is promising *in vivo* tool in various biomedical applications; moreover, in recent years, its use for characterizing articular cartilage degeneration has been developing. It has also shown potential for scoring the severity of cartilage lesions, which could be useful in determining the optimal treatment strategy during cartilage repair surgery. However, the effect of different cartilage injury types on Raman spectra is unknown. This study aims to investigate the potential of Raman spectroscopy for detecting changes in cartilage due to different injury types. Artificial injuries were induced in cartilage samples using established mechanical and enzymatic approaches to mimic trauma-induced and natural degeneration. Mechanical damage was induced using surface abrasion (ABR, $n = 12$) or impact loading (IMP, $n = 12$), while enzymatic damage was induced using three different treatments: 30 min trypsin digestion (T30, $n = 12$), 90 min collagenase digestion (C90, $n = 12$), and 24 h collagenase digestion (C24, $n = 12$). Raman spectra were obtained from all specimens, and partial least squares discriminant analysis (PLS-DA) was used to distinguish cartilage injury types from their respective controls. PLS-DA cross-validation accuracies were higher for C24 (88%) and IMP (79%) than for C90 (67%), T30 (63%), and ABR (58%) groups. This study indicates that Raman spectroscopy, combined with multivariate analysis, can discern different cartilage injury types. This knowledge could be useful in clinical decision-making, for example, selecting the optimal treatment remedy during cartilage repair surgery.

KEYWORDS

cartilage degeneration, multivariate analysis, osteoarthritis, PLS-DA, Raman spectroscopy

This is an open access article under the terms of the Creative Commons Attribution License, which permits use, distribution and reproduction in any medium, provided the original work is properly cited.

© 2021 The Authors. *Journal of Raman Spectroscopy* published by John Wiley & Sons Ltd.

1 | INTRODUCTION

Articular cartilage (AC) is a specialized connective tissue that allows near frictionless movement of joints.^[1] AC is an avascular and aneural tissue consisting predominantly of water (65%–80%), collagen (10%–30%), and proteoglycans (3%–10%).^[1] Due to the limited regenerative capacity of AC, it is susceptible to progressive degeneration after an initial injury.^[2] Impact injury on the joint can lead to a degenerative joint condition known as post-traumatic osteoarthritis (PTOA), which in its advanced stage is characterized by erosion of cartilage matrix, joint pain, and restricted mobility.^[3] Hence, it is critical to diagnose joint damage at an early stage where matrix degeneration may be halted or even reversed using pharmaceutical or surgical interventions.^[3–5] Cartilage injury can be evaluated and repaired during arthroscopic surgery. However, conventional arthroscopy suffers from poor diagnostic reproducibility and lacks reliable quantitative and objective information.^[6,7] It has been suggested that the reliability and objectivity of arthroscopic evaluation can be improved by complementary quantitative diagnostic optical techniques—such as near-infrared spectroscopy, Fourier-transform infrared spectroscopy (FTIR), Raman spectroscopy, and optical coherence tomography. These methods can be adapted in a minimally invasive approach for nondestructive, sensitive, and objective assessment of cartilage integrity.^[8–12] Furthermore, Raman spectroscopy is also a potential technique for quantitative arthroscopic evaluation of joint tissues.^[13–21]

Raman spectroscopy is based on inelastic scattering (*i.e.*, Raman scattering) of light, enabling assessment of the biochemical composition and, thus, the integrity of biological tissues.^[22] Initially, after the discovery of Raman scattering, the major limiting factor for the implementation of Raman spectroscopy in biomedicine was the weak scattering signals.^[23] Nevertheless, the invention of the laser in the 1960s and application of fiber optics and charge-coupled devices (CCDs) in the 1980s has rapidly increased the popularity of Raman spectroscopy in biomedical research.^[13,23,24] In the last decades, Raman spectroscopy has proved to be a promising tool for characterizing biomolecular changes in tissue composition related to various diseases.^[13,18,23–25] In comparison with other vibrational spectroscopic techniques, Raman spectroscopy encounters less interference from water in the biological fingerprint region (800^{-1} – 1800 cm^{-1}).^[16] This asset makes Raman spectroscopy particularly suitable for the characterization of biomolecular changes in biological tissues, such as AC, which consists of 65%–80% water.^[1,16]

Raman spectroscopy has been shown to be a potential technique for quantifying cartilage properties.^[18] The study explored its potential for arthroscopic assessment of AC.^[14] In the same year, Raman spectroscopy was shown to be capable of detecting biomolecular changes associated with impact-related cartilage damage.^[16] Subsequently, it was also suggested that Raman spectroscopy has the potential for diagnosing cartilage damage, as well as monitoring subchondral bone integrity in pathogenesis related to osteoarthritis (OA).^[19] Moreover, a Raman band that might be useful for the determination of proteoglycans in cartilage and bone was identified.^[15] Molecular information derived from Raman spectroscopy could be linked with the conventional Collins scale, providing a potential nondestructive approach for pathological grading of cartilage and subchondral bone changes in OA.^[20] Additionally, it has been demonstrated that Raman spectroscopy can detect depth-dependent changes in bovine cartilage after a wear test.^[21] Finally, it has been shown that Raman bands at high wavenumbers ($3,000$ – $3,800\text{ cm}^{-1}$) are associated with water content, which has a significant correlation with the mechanical properties of human cartilage.^[26]

Based on the literature, Raman spectroscopy can identify biochemical changes in cartilage matrix due to mechanical damage;^[16,21] however, changes in the Raman spectrum related to selective enzymatic degradation have not been thoroughly investigated. This information related to various kinds of cartilage injuries could be crucial when selecting the optimal treatment methods during arthroscopic cartilage repair surgery. However, the sensitivity of Raman spectroscopy to different types of cartilage pathology needs to be further investigated before exploring its full potential in the arthroscopic characterization of cartilage integrity. We hypothesize that Raman spectroscopy can detect biochemical changes associated with cartilage injuries induced mechanically or enzymatically, which mimic post-traumatic and idiopathic OA, respectively.

The validity of this hypothesis was investigated experimentally using samples with various types of mechanical and enzymatic degeneration. Mechanical damage was induced through surface abrasion (ABR) or impact loading (IMP), whereas enzymatic damage was caused using three different treatments—30 min trypsin digestion (T30), 90 min collagenase digestion (C90), and 24 h collagenase digestion (C24). Raman spectra were measured from the specimens, and partial least squares discriminant analysis (PLS-DA) was carried out to differentiate damaged samples from their controls, as well as to differentiate between injury types, based on spectral variations resulting from the different cartilage injuries (Figure 1).

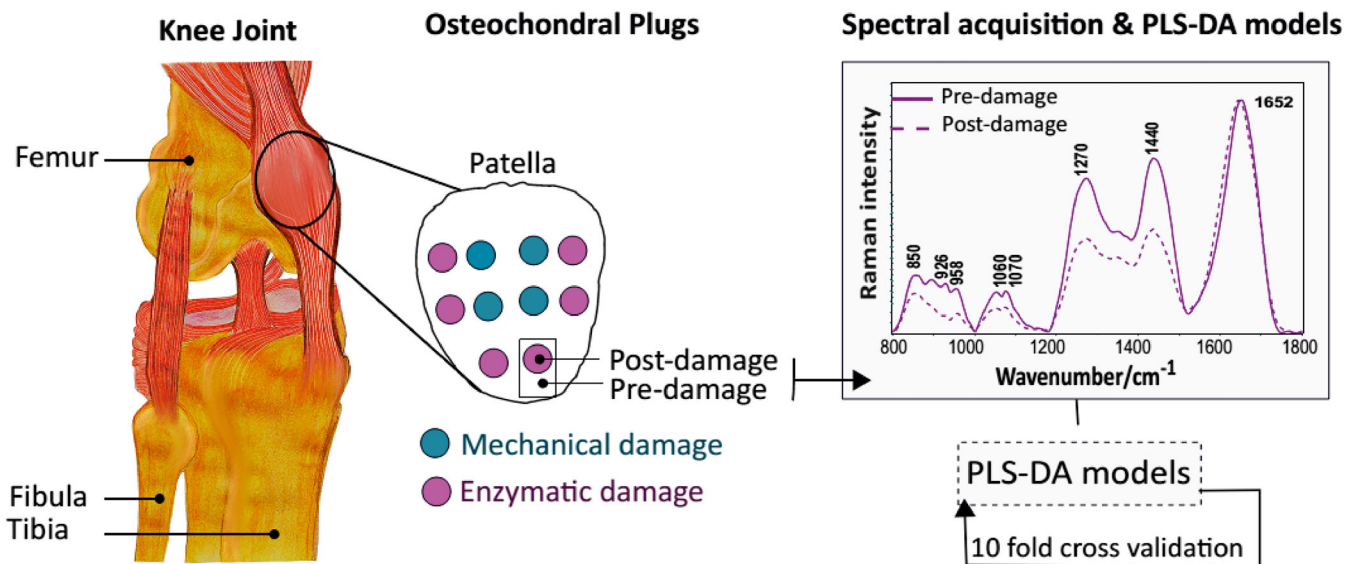


FIGURE 1 Study protocol

2 | MATERIALS AND METHODS

2.1 | Sample preparation

Patellae ($n = 10$) were extracted from fresh bovine (age 14–22 months) knee joints obtained from a local slaughterhouse, and therefore, no ethical permission was required. Osteochondral specimens ($n = 60$) were extracted from different anatomical locations of the lateral and medial patellae without any signs of natural damage on the cartilage surface. One-half of each specimen was used as a pre-damage group, and the other half was utilized for post-damage (mechanically or enzymatically degraded cartilage) experiments (Figure 1). All the specimens (pre- and post-damage specimens) were stored in phosphate-buffered saline (PBS) between the preparation steps and the Raman spectra measurements step.

Pre- and post-damage specimens for each group were extracted from the same anatomical location to avoid variations based on the specimen's location on the patella. In the case of mechanical damage, cylindrical osteochondral specimens ($diameter = 7$ mm) were prepared, whereas enzymatic degradation was carried out on larger tissue samples. Larger samples were utilized to avoid lateral penetration of enzyme into the sample. After the enzymatic treatment, cylindrical plugs ($diameter = 7$ mm) were extracted, and Raman spectra were acquired from the region of interest. Specimens were always immersed in PBS before and after measurements. After spectral measurements, the specimens were formalin fixed, decalcified in ethylenediaminetetraacetic acid (EDTA), and then embedded in paraffin.

Histological sections ($thickness = 3$ μ m) were cut and stained using Safranin-O, a stain that binds stoichiometrically with matrix proteoglycans. Digital images were acquired from the histological sections using a PathScanEnabler-IV (MeyerInstruments, Inc., USA).

Mechanical damage was induced on the cylindrical osteochondral specimens via impact loading (IMP, $n = 12$) or surface abrasion (ABR, $n = 12$). Surface abrasion and impact damage were created following the protocol described in earlier studies (Figure 2).^{9,11} A custom-made drop tower was used to create an impact injury on the specimens (Figure 2b).¹¹ Impact loading was carried out using a stainless steel impactor (200 g) with a polished steel ball ($diameter = 1$ cm) at the impact surface. The impactor was dropped from a height of 7.5 cm. The impactor height, and thus, energy delivered to the cartilage surface, was determined based on preliminary assessments to create minor cracks on the cartilage surface. A customised setup (Figure 2a) was used to induce abrasive damage on the cartilage surface.⁹ Specimen surface was abraded under constant stress (4 kPa) by a rotating metal plate (180°) covered with sandpaper (P80, 200 μ m particle size). This procedure was repeated in two perpendicular directions. Immediately after this protocol, specimens were rinsed in PBS, and subsequently, their Raman spectra were acquired.

2.2 | Enzymatic degradation

Enzymatic degradation of specimens ($n = 36$) was conducted using either collagenase or trypsin. Collagenase D (0.1 mg/ml, Sigma-Aldrich Inc., St. Louis, MO, USA) was

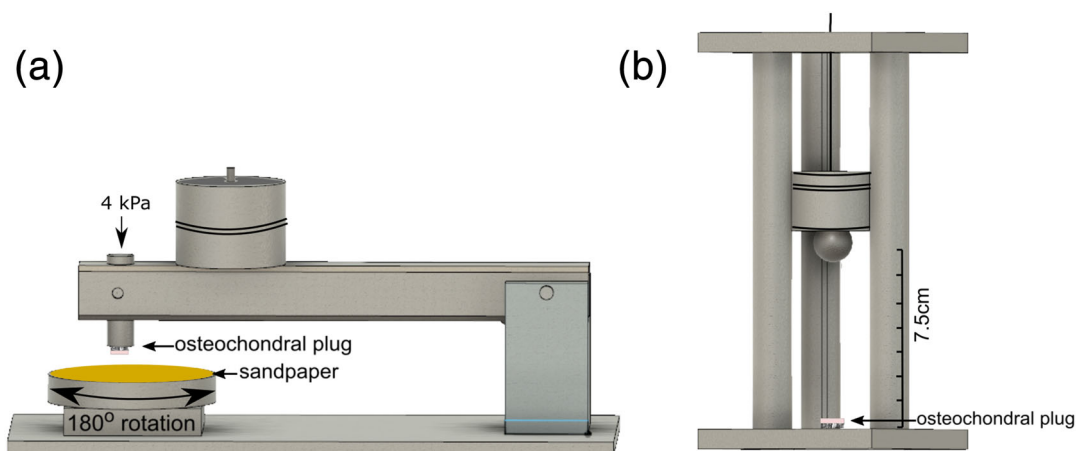


FIGURE 2 (a) Custom-made tool for inducing surface abrasion on cartilage. (b) Custom-made drop tower to create impact injury

utilized for digestion of the collagen network, whereas trypsin (0.5 mg/ml, T4299, Sigma-Aldrich Inc., St. Louis, MO, USA) was used to deplete the proteoglycans from the extracellular matrix.^{27,28} Collagenases D explicitly targets and cleaves the collagen molecules in the triple helix region, whereas trypsin cuts the peptide bond on the C-terminal side of lysine and arginine amino acids (Sigma-Aldrich Inc).

Prior to enzymatic degradation, the specimens were subdivided into three groups: collagenase 24 h (C24, $n = 12$), collagenase 90 min (C90, $n = 12$), and trypsin 30 min (T30, $n = 12$). Specimens were incubated at 37°C and 5% CO₂ in PBS solution containing the respective enzymes with supplementary antibiotics (Penicillin–Streptomycin–Amphotericin B, 100 units/ml penicillin, 100 µg/ml streptomycin, and 0.25 µg/ml amphotericin B, Sigma-Aldrich Inc., St. Louis, MO, USA).²⁹ For mild cartilage degradation, we applied a shorter incubation time of 30 min for trypsin (T30) and 90 min for collagenase (C90). A long incubation time of 24 h was also applied with collagenase (C24) to induce severe damage. After enzymatic treatment, specimens were rinsed in PBS before the Raman spectroscopic measurements.

2.3 | Raman spectroscopy

Raman spectra were acquired from the center of each osteochondral specimen three times. A total of 360 spectra from 60 damage (post-damaged) and 60 normal (pre-damaged) specimens were measured. Raman confocal microscope (Thermo Fisher Scientific DXR2xi, Madison, WI, USA) in the range of 200–3,400 cm⁻¹ with 785 nm laser at 30 mW through a 10x objective, with a 50 µm confocal pinhole, 0.5 s exposure time, and 120 accumulation was used.

2.4 | Data pre-processing and multivariate analysis

Multivariate data analysis was carried out on pre-processed spectra. Pre-processing of the acquired spectral data was consistent with a previously established protocol.^{30,31} The spectral pre-processing procedure was conducted using an open-source toolbox (<https://github.com/uef-bbc/nippy>).³² Pre-processing included the following: (1) background subtraction, (2) interpolation (800–1,800 cm⁻¹ range), (3) baseline correction, and (4) SNV (standard normal variate) normalization.

PLS-DA was carried out to classify the cartilage samples into pre- versus post-damage groups. The investigation was based solely on the Raman spectral data and performed using a classification toolbox (version 5.3) in MATLAB (MathWorks Inc, Natick, MA, USA).³³ PLS-DA models were developed to classify pre- versus post-damaged specimens of different injury types. Due to the relatively small sample size, 10-fold cross-validation was used during development of the PLS-DA models. The performance of the models was evaluated based on cross-validated error rates.

3 | RESULTS

The mean Raman spectra (background and baseline corrected) of all groups showed significant peaks at 1,652, 1,440, and 1,270 cm⁻¹ and minor peaks at 1,070, 1,060, 958, 926, and 850 cm⁻¹ (Figures 3 and S2). These features correspond to the vibrational modes of collagen, glycosaminoglycan (GAGs), and bone (Table S1). We observed the most significant spectral differences between pre- versus post-damage in C24 and IMP groups (Figure 3). We also noticed subtle spectral differences at 1,652,

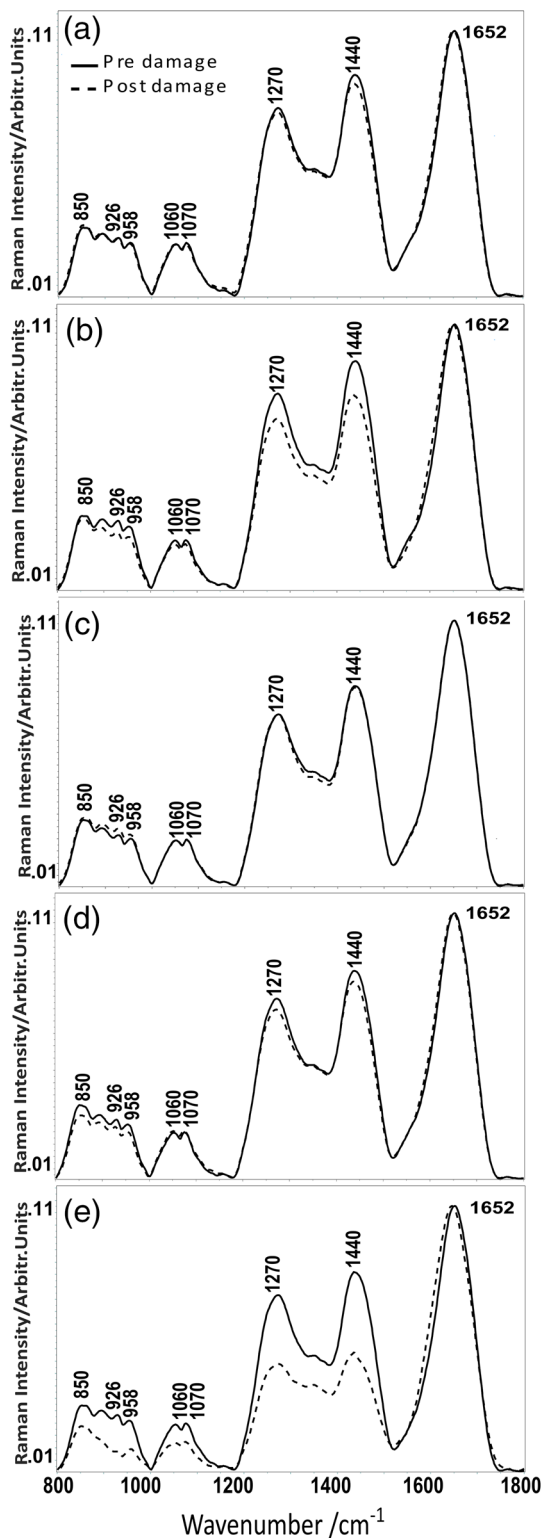


FIGURE 3 Mean Raman spectra of pre- versus post-cartilage damage (a) ABR (abrasion), (b) IMP (impact), (c) T30 (trypsin 30 min), (d) C90 (collagenase 90 min), and (e) C24 (collagenase 24 h)

1,440, 1,270, and 800–1,100 cm^{-1} between pre-ABR versus post-ABR and C90 groups. Besides, we observed minor differences in the 850–1,000 cm^{-1} range due to trypsin degeneration (T30).

The PLS-DA calibration models had accuracies ranging between 81% and 100%, with cross-validation accuracies ranging between 58% and 88% (Table 1). The best cross-validated accuracies were obtained between pre-C24 and post-C24 (88%) and among pre-IMP and post-IMP (79%) groups. PLS-DA classification accuracy for the “pre- versus post-cartilage damage” group was 74% (Figure 4a). In contrast, the classification models that discriminated mechanical and enzymatic damage from their respective controls showed classification accuracies of 81% and 76%, respectively (Figure 4b).

Images of Safranin-O stained sections show that samples with ABR and impact damage have irregular cartilage surface and chondral cracks, respectively (Figure S1). We observed marginally reduced Safranin-O staining (*i.e.*, mild proteoglycan loss) in the case of C90 and T30 groups. In the case of the C24 group, we noticed disorganization of cartilage in the superficial and middle zones with a significant reduction in safranin-O staining (*i.e.*, severe proteoglycan loss).

4 | DISCUSSION

In the present study, we investigated the capability of Raman spectroscopy to detect changes in cartilage composition induced by mechanical or enzymatic degradation, mimicking post-traumatic and idiopathic OA, respectively. The mean Raman spectra of nondamaged cartilage revealed molecular vibrations corresponding to amide I, δ CH_2 stretch, amide III, carbonate stretch, SO_3^- symmetric stretch, PO_4^{3-} phosphate stretch, proline, and hydroxyproline (Table S1). These observations are in line with literature suggesting that molecular vibrations from collagen, GAGs, and bone dominate Raman spectra recorded from osteochondral specimens.^{14,17,19} The substantial differences in Raman spectral features between pre- and post-damage in C24 and IMP groups are due to the injury-related disruption in biochemical structure and composition. The mean Raman spectrum of the C24 group (Figure 3) exhibited a blue shift in the amide I peak from 1,652 to 1,642 cm^{-1} ; the change in the amide I can be attributed to secondary structural deformation of collagen. This shift in the amide I could not be assigned to proteoglycans as it was not observed in the T30 group. We notice a similar but more subtle change in the amide I peak of the C90 group. To the best of our knowledge, this has not been reported earlier.

Raman spectra displayed significant intensity-related variations in amide III and δ CH_2 stretch in an impact injury group. Earlier, the red-shift from 1,264 to 1,274 cm^{-1} after impact damage in porcine cartilage has been reported.¹⁶ It was proposed that this shift in

TABLE 1 PLS-DA analysis for (A) pre- (ABR_{pre}) versus post- (ABR_{post}) abrasion, (B) pre- (IMP_{pre}) versus post- (IMP_{post}) impact, (C) pre- (T30_{pre}) versus post- (T30_{post}) trypsin 30 min, (D) pre- (C90_{pre}) versus post- (C90_{post}) collagenase 90 min, (E) pre- (C24_{pre}) versus post- (C24_{post}) collagenase 24 h, (F) pre- (M_{pre}) versus post- (M_{post}) mechanical damage, (G) pre- (E_{pre}) versus post- (E_{post}) enzymatic damage, (H) enzymatic damage (E_{post}) versus mechanical damage (M_{post}), and (I) pre- (D_{pre}) versus post- (D_{post}) “damage” group

Partial least squares discriminant analysis (PLS-DA)		Number of LV	Sensitivity (%)	Specificity (%)	Accuracy (%)
(A) ABR _{pre} versus ABR _{post}	Calibration model	4	83	92	91
	Cross-validation		67	50	58
(B) IMP _{pre} versus IMP _{post}	Calibration model	4	100	100	100
	Cross-validation		83	75	79
(C) T30 _{pre} versus T30 _{post}	Calibration model	4	83	92	88
	Cross-validation		58	67	63
(D) C90 _{pre} versus C90 _{post}	Calibration model	4	92	83	88
	Cross-validation		58	75	67
(E) C24 _{pre} versus C24 _{post}	Calibration model	3	92	92	92
	Cross-validation		92	83	88
(F) M _{pre} versus M _{post}	Calibration model	8	96	83	90
	Cross-validation		83	79	81
(G) E _{pre} versus E _{post}	Calibration model	8	83	92	88
	Cross-validation		81	72	76
(H) E _{post} versus M _{post}	Calibration model	8	92	92	92
	Cross-validation		75	79	77
(I) D _{pre} versus D _{post}	Calibration model	8	87	75	81
	Cross-validation		82	67	74

Note: The bold number in the table is to emphasize the description in the results section. It will help the readers to have smooth access to the information.

amide III was due to compression of C-N vibration in collagen fibers.¹⁶ In the current study, we noticed intensity-related variations in the amide III peak. These changes in amide III peak intensity are potentially due to the conformational, and configuration change in the collagen macromolecules as well as depletion of proteoglycans (Figure S1). We observed subtle but significant changes in amide III and δ CH₂ peaks in the Raman spectra of the ABR group. These observations are also consistent with an earlier study.²¹ The mean Raman spectrum of the T30 group exhibited minor variation in δ CH₂ stretch and amide III peak. We did not observe any differences at 1,060 cm⁻¹ (SO₃-symmetric stretch)—the molecular vibration assigned to chondroitin sulfate. These findings could be due to trypsin targeting the peptide bonds rather than the chondroitin chain.²²

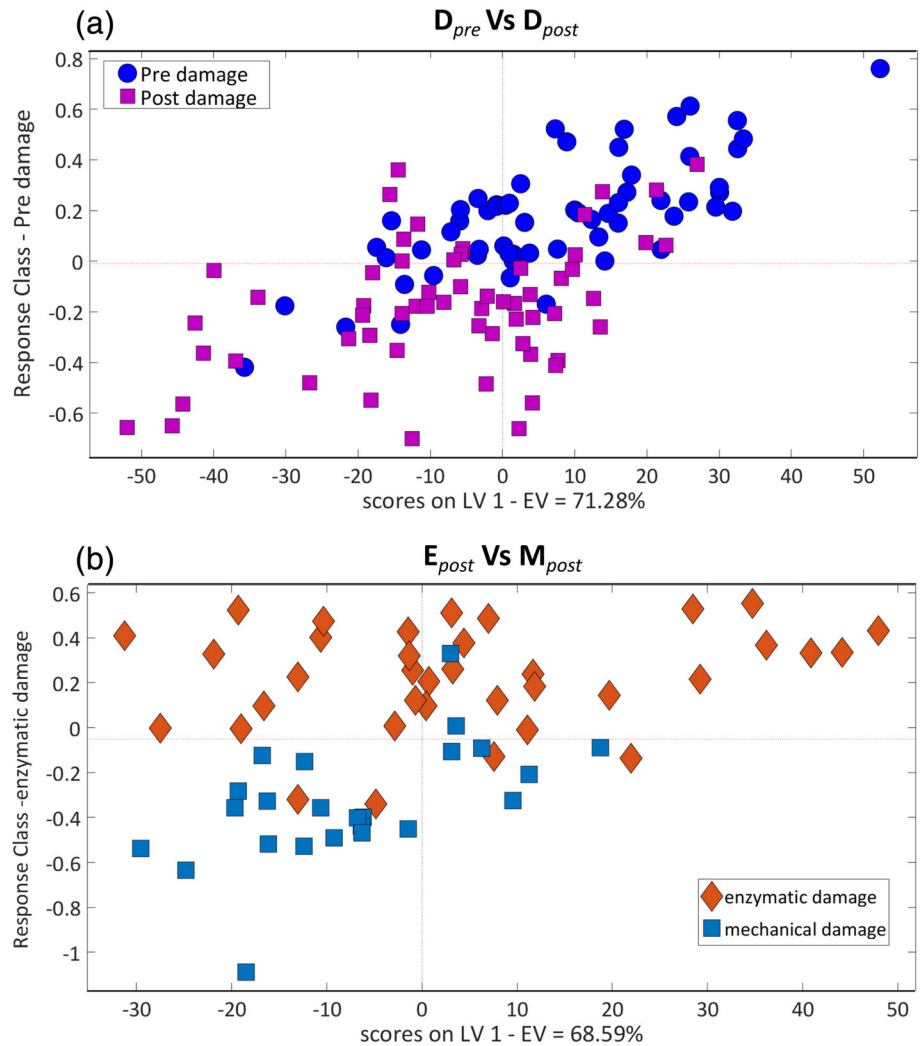
To investigate the statistical significance of Raman spectral variance induced by mechanical or enzymatic damage, PLS-DA was carried out. PLS-DA is a linear discriminant analysis that extends the properties of partial least squares regression to classification. In the current study, the observed classification accuracy was directly proportional to the severity of the cartilage

damage (Table 1). Thus, the classification accuracy for pre- versus post-damage was highest for C24 and lowest for the ABR group. The low cross-validation accuracy of 58% observed in the case of ABR group is likely due to mild surface damage. It is widely thought that proteases-mediated degradation of cartilage matrix is a fundamental feature of idiopathic OA.³⁴

In contrast, mechanical damage induces structural changes in cartilage matrix, leading to PTOA.^{3,35} Based on these facts, we combined the spectra from ABR and IMP groups into mechanical damage group and T30, C90, and C24 groups into enzymatic damage group. We further pooled the spectra from mechanical and enzymatic degraded specimens into the “pre-damage (D_{pre}) versus post-damage (D_{post})” group and observed that PLS-DA had a classification accuracy of 74% (Figure 4a). Moreover, we observed relatively similar classification accuracies for pre- versus post-damage for mechanical damage (81%) and enzymatic damage (76%) groups. The confusion matrix of 10-fold cross-validation for the PLS-DA analysis is presented in Table 2.

Safranin-O stain binds to matrix proteoglycans in cartilage tissue, and decrease in the intensity of the stain on histological slides is related to the loss of

FIGURE 4 Scatter plots for PLS-DA analysis (a) pre- (D_{pre}) versus post- (D_{post}) “damage” group (b) enzymatic (E_{post}) versus mechanical (M_{post}) damage



proteoglycans. Superficial cartilage damage was evident in C90 and T30 groups based on Safranin-O stained sections (Figure S1), which displayed minor loss of proteoglycans indicated by the slightly reduced stain intensity. The ABR group showed a discontinuous surface with no significant decrease in stain intensity. The C24 group exhibits evident disorganization of the articular surface, resulting from superficial collagen disruption along with collateral loss of proteoglycans indicated by the reduced stain intensity at the superficial and mid-layers of the tissue. These observations are supported by earlier studies.^{9,36} In the case of the IMP group, chondral cracks with a slight loss of stain intensity in superficial cartilage could be observed, suggesting a loss of proteoglycans.

There are certain limitations related to the study setup. One of the potential limitations is associated with instrumentation. Raman spectral measurements were acquired using Raman microscopic system rather than a fiber optic-based *in vivo* system, possibly resulting in a smaller sampling area and lower quality of spectra. The

second limitation is related to the limited number of osteochondral samples. However, preliminary analysis and previous studies suggest that the sample size used in the study was sufficient to test the present hypothesis.^{15,19–21} Nevertheless, these limitations do not alter the underlying findings and conclusions of the present study. This study demonstrated that Raman spectroscopy has the potential to detect biochemical changes associated with different cartilage injury types.

In the past few years, vibrational (mid-infrared, near-infrared and Raman) spectroscopy has evolved as a promising *in vivo* tool in various biomedical applications including cartilage research. These techniques have also shown potential for scoring the severity of cartilage lesions, which can be useful in determining the optimal treatment strategy during cartilage repair surgery. Efforts are ongoing to develop mid-infrared and near-infrared-based probes for arthroscopic evaluation of connective tissue integrity during repair surgery. Currently, the utility of *in vivo* fiber optic-based Raman spectroscopy probes in cancer is well established. However, to our knowledge,

TABLE 2 Confusion matrix of 10-fold cross-validation for PLS-DA

(a) Mechanical (M) damage group		
	M_{pre} (%)	M_{post} (%)
M_{pre} (%)	83	17
M_{post} (%)	21	79
(b) Enzymatic (E) damage group		
	E_{pre} (%)	E_{post} (%)
E_{pre} (%)	81	19
E_{post} (%)	28	72
(c) Enzymatic (E) versus mechanical (M) damage		
	E_{post} (%)	M_{post} (%)
E_{post} (%)	75	25
M_{post} (%)	21	79
(d) Pre-damage (D_{pre}) versus post-damage (D_{post}) groups		
	D_{pre} (%)	D_{post} (%)
D_{pre} (%)	82	18
D_{post} (%)	33	67

Note: The bold number in the table is to emphasize the description in the results section. It will help the readers to have smooth access to the information.

there is no Raman spectroscopy-based probe for arthroscopic applications. This is due to the limited body of work on applicability of Raman spectroscopy in musculoskeletal research. Moreover, it is challenging to develop Raman spectroscopy-based hook-shaped probes for arthroscopic applications. Further research and efforts to solve these challenges are required.

5 | CONCLUSIONS

The capability of Raman spectroscopy to differentiate cartilage injuries that mimic post-traumatic and idiopathic OA by mechanically and enzymatically induced damages, respectively, was investigated. It was found that Raman spectroscopy in combination with multivariate analysis can discern different cartilage injury types. This information is critical and could be useful in clinical decision-making, for example, when selecting the optimal treatment remedy during cartilage repair surgery.

ACKNOWLEDGEMENTS

The MIRACLE project-Horizon 2020 research and innovation programme-H2020-ICT-2017-1 (grant agreement 780598), Academy of Finland (project 315820), Kuopio University Hospital (VTR project 5203111), and Doctoral

Programme in Science, Technology, and Computing (SCITECO) of the University of Eastern Finland financially supported this study.

CONFLICT OF INTEREST

The authors have no conflicts of interest to declare.

ORCID

Rubina Shaikh  <https://orcid.org/0000-0003-4184-8254>

Ervin Nippolainen  <https://orcid.org/0000-0002-1317-2683>

Vesa Virtanen  <https://orcid.org/0000-0002-5797-5365>

Jari Torniaainen  <https://orcid.org/0000-0003-4953-4508>

Lassi Rieppo  <https://orcid.org/0000-0001-5542-4060>

Simo Saarakkala  <https://orcid.org/0000-0003-2850-5484>

Isaac O. Afara  <https://orcid.org/0000-0001-7114-0439>

Juha Töyräs  <https://orcid.org/0000-0002-8035-1606>

REFERENCES

- [1] A. J. Sophia Fox, A. Bedi, S. A. Rodeo, *Sport. Heal. A Multidiscip. Approach* **2009**, *1*, 461.
- [2] W. Zhang, H. Ouyang, C. R. Dass, J. Xu, *Bone Res.* **2016**, *4*, 15040.
- [3] T. S. Ali, I. Prasadam, Y. Xiao, K. I. Momot, *Sci. Rep.* **2018**, *8*, 6861.
- [4] A.-C. Bay-Jensen, S. Hoegh-Madsen, E. Dam, K. Henriksen, B. C. Sondergaard, P. Pastoureau, P. Qvist, M. A. Karsdal, *Rheumatol. Int.* **2010**, *30*, 435.
- [5] S. A. Olson, B. D. Furman, V. B. Kraus, J. L. Huebner, F. Guilak, *J. Orthop. Res.* **2015**, *33*, 1266.
- [6] B. H. Brismar, T. Wredmark, T. Movin, J. Leandersson, O. Svensson, J. Bone Joint, *Surg. Br.* **2002**, *84*, 42.
- [7] G. Spahn, H. M. Klinger, M. Baums, U. Pinkepank, G. O. Hofmann, *Arch. Orthop. Trauma Surg.* **2011**, *131*, 377.
- [8] M. Prakash, A. Joukainen, J. Torniaainen, M. K. M. Honkanen, L. Rieppo, I. O. Afara, H. Kröger, J. Töyräs, J. K. Sarin, *Osteoarthr. Cartil.* **2019**, *27*, 1235.
- [9] S. Saarakkala, J. Toyras, J. Hirvonen, M. S. Laasanen, R. Lappalainen, J. S. Jurvelin, *Ultrasound Med. Biol.* **2004**, *30*, 783.
- [10] J. K. Sarin, O. Nykänen, V. Tiitu, I. A. D. Mancini, H. Brommer, J. Visser, J. Malda, P. R. van Weeren, I. O. Afara, J. Töyräs, *Ann. Biomed. Eng.* **2019**, *47*, 1815.
- [11] A. E. A. Saukko, J. T. J. Honkanen, W. Xu, S. P. Vaananen, J. S. Jurvelin, V.-P. Lehto, J. Toyras, *Ann. Biomed. Eng.* **2017**, *45*, 2857.
- [12] P. H. Puhakka, N. C. R. Te Moller, P. Tanska, S. Saarakkala, V. Tiitu, R. K. Korhonen, H. Brommer, T. Virén, J. S. Jurvelin, J. Töyräs, *Acta Orthop.* **2016**, *87*, 418.
- [13] D. I. Ellis, D. P. Cowcher, L. Ashton, S. O'Hagan, R. Goodacre, *Analyst* **2013**, *138*, 3871.
- [14] K. A. Esmonde-White, F. W. L. Esmonde-White, M. D. Morris, B. J. Roessler, *Analyst* **2011**, *136*, 1675.
- [15] S. Gamsjaeger, K. Klaushofer, E. P. Paschalis, *J. Raman Spectrosc.* **2014**, *45*, 794.

- [16] N. S. J. Lim, Z. Hamed, C. H. Yeow, C. Chan, Z. Huang, *J. Biomed. Opt.* **2011**, *16*, 17003.
- [17] W. Richardson, D. Wilkinson, L. Wu, F. Petrigliano, B. Dunn, D. Evseenko, *J. Biophotonics* **2015**, *8*, 555.
- [18] L. Rieppo, J. Töyräs, S. Saarakkala, *Appl. Spectrosc. Rev.* **2017**, *52*, 249.
- [19] R. A. de Souza, M. Xavier, N. M. Manguiera, A. P. Santos, A. L. B. Pinheiro, A. B. Villaverde, L. J. Silveira, *Lasers Med. Sci.* **2014**, *29*, 797.
- [20] Y. Takahashi, N. Sugano, M. Takao, T. Sakai, T. Nishii, G. Pezzotti, *J. Mech. Behav. Biomed. Mater.* **2014**, *31*, 77.
- [21] L. Tong, Z. Hao, C. Wan, S. Wen, *J. Biophotonics* **2018**, *11*, e201700217.
- [22] M. B. Albro, M. S. Bergholt, J. P. St-Pierre, A. Vinals Guitart, H. M. Zlotnick, E. G. Evita, M. M. Stevens, *npj Regen. Med.* **2018**, *3*(3).
- [23] D. W. Shipp, F. Sinjab, I. Notingher, *Adv. Opt. Photonics* **2017**, *9*, 315.
- [24] E. Cordero, I. Latka, C. Matthäus, I. W. Schie, J. Popp, *J. Biomed. Opt.* **2018**, *23*, 1.
- [25] R. Shaikh, M. Chilakapati, *J. Cancer Res. Ther.* **2015**, *11*, 10.
- [26] M. Unal, O. Akkus, J. Sun, L. Cai, U. L. Erol, L. Sabri, C. P. Neu, *Osteoarthr. Cartil.* **2019**, *27*, 304.
- [27] W. D. Shingleton, D. J. Hodges, P. Brick, T. E. Cawston, *Biochem. Cell Biol.* **1996**, *74*, 759.
- [28] E. D. J. Harris, H. G. Parker, E. L. Radin, S. M. Krane, *Arthritis Rheum.* **1972**, *15*, 497.
- [29] J. Toyra, M. S. Laasanen, S. Saarakkala, M. J. Lammi, J. Rieppo, J. Kurkijarvi, R. Lappalainen, J. S. Jurvelin, *Ultrasound Med. Biol.* **2003**, *29*, 447.
- [30] A. Nijssen, K. Maquelin, L. F. Santos, P. J. Caspers, T. C. Bakker Schut, J. C. den Hollander, M. H. A. Neumann, G. J. Puppels, *J. Biomed. Opt.* **2007**, *12*, 34004.
- [31] H. J. Butler, L. Ashton, B. Bird, G. Cinque, K. Curtis, J. Dorney, K. Esmonde-White, N. J. Fullwood, B. Gardner, P. L. Martin-Hirsch, M. J. Walsh, M. R. McAinsh, N. Stone, F. L. Martin, *Nat. Protoc.* **2016**, *11*, 664.
- [32] J. Torniaainen, I. O. Afara, M. Prakash, J. K. Sarin, L. Stenroth, J. Töyräs, *Biophotonics Congress: Optics in the Life Sciences Congress 2019 (BODA, BRAIN, NTM, OMA, OMP)*, Optical Society of America, Tucson, Arizona **2019** DS2A.6.
- [33] D. Ballabio, V. Consonni, *Anal. Methods* **2013**, *5*, 3790.
- [34] L. Troeberg, H. Nagase, *Biophys. Acta - Proteins Proteomics* **1824**, *2012*, 133.
- [35] M. E. Cooke, B. M. Lawless, S. W. Jones, L. M. Grover, *Acta Biomater.* **2018**, *78*, 320.
- [36] J. Rieppo, J. Toyra, M. T. Nieminen, V. Kovanen, M. M. Hyttinen, R. K. Korhonen, J. S. Jurvelin, H. J. Helminen, *Cells. Tissues. Organs* **2003**, *175*, 121.

SUPPORTING INFORMATION

Additional supporting information may be found online in the Supporting Information section at the end of this article.

How to cite this article: Shaikh R, Nippolainen E, Virtanen V, et al. Raman spectroscopy is sensitive to biochemical changes related to various cartilage injuries. *J Raman Spectrosc.* 2021;1–9. <https://doi.org/10.1002/jrs.6062>